Supplementary Material

Dynamic generation of power function gradient profiles in a universal microfluidic gradient generator by controlling the inlet flow rates

Gauri Paduthol [1,2], Teji Shenne Korma [1], Amit Agrawal [2], Debjani Paul [1,*]

[1] Department of Bioscience and Bioengineering, Indian Institute of Technology Bombay, Powai, Mumbai 400076

[2] Department of Mechanical Engineering, Indian Institute of Technology Bombay, Powai, Mumbai 400076

[*] Email for correspondence: debjani.paul@iitb.ac.in

1. Impact of length of barrier overlap on the accuracy of the gradient generated

The barrier overlaps have been designed to (a) reduce flow reversal observed between the transition from one level to the next and (b) to reduce the lateral diffusion of dye between channels of the same level. As both of these are spatially local phenomena, targeted at the level changes, we would expect that increasing the length of barrier overlap from 0µm would decrease the error between required and expected profiles. Increasing barrier overlap length would break the incoming flows before interacting with each other. But as the length of the barrier overlap increases, we will reach a point where both these spatially local phenomena become redundant in comparison to point at which the inlet flows are divided and thus do not impact the gradient formed at the output. Once this stage is reached, increasing the barrier overlap length any further would not impact/ improve the error observed in any way.

To proof this hypothesis, we conducted a few simulations as suggested to develop a gradient profile for $y = x^{0.5}$ at the outlet, while changing the length of the barrier overlap from 0 µm to 200 µm at intervals of 25 µm. All other dimensions were kept the same as mentioned previously in the manuscript. The inlet conditions were kept the same throughout i.e., $n = 2.15$, $m = 6 \times 10^{-6}\, m/s$. As seen in **figure S1**, we see that the error decreases with increasing barrier length till approximately 50 µm and then essentially stagnates as expected. This suggests that the overlap of barriers is an important design parameter, which needs to be carefully optimized.

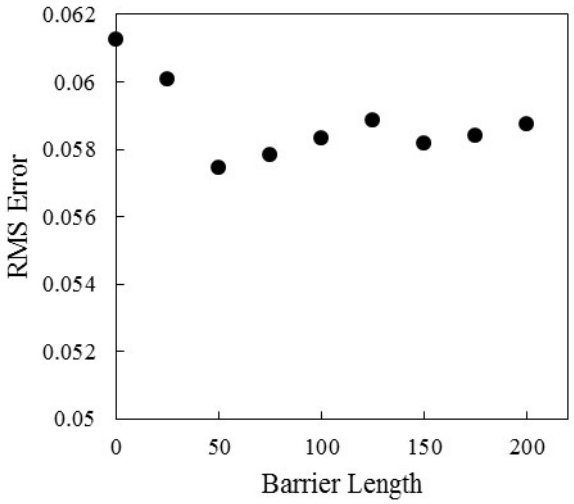

Figure S1: Variation of RMS error of the gradient generated wrt increasing barrier overlap length between level 1 and level 2. The simulations were conducted with the same conditions, at $n = 2.15$, $m = 6 \times 10^{-6}\, m/s$, to generate $y = x^{0.5}$ at the outlet.

2. Schematic diagram of the experimental device

The experiments were conducted on a device with larger dimensions than that used in simulations as mentioned in the section '*Device Design'.* This was to accommodate complete mixing in the device based on the flowrates achievable by our experimental setup. **(figure**

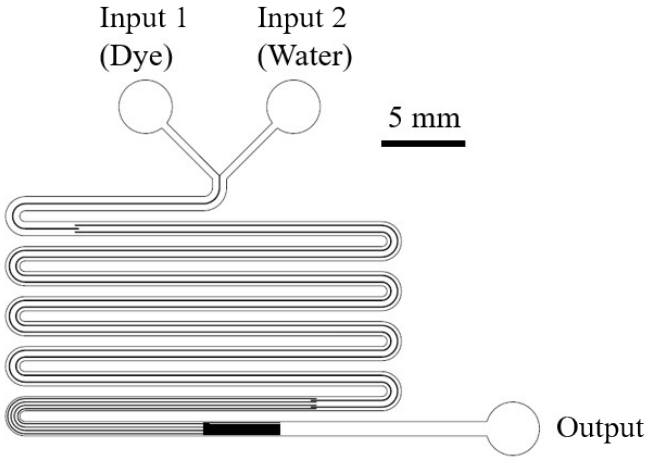

Figure S2: A schematic diagram of the device used to conduct experiments. The length and width for each level is mentioned in the *'Device Design'* section.

S2)

3. Comparison of flat flow profile and parabolic flow profile

As detailed before, α and β are the percentage volumetric flow corresponding to the channel i, j and channel $i-1, j$ that flows into channel $2i-2, j+1$. The values of of α and β in equations (1) – (4) are defined for each iteration based on the corresponding position of barriers and the velocity profiles. Consider an iteration to calculate the concentration in channel $(2i-2)$, $(j+1)$. Let the width of the channel i, j be represented as $w_{i,j} = u_{i,j} - u_{i-1,j}$. Let the section of $w_{i,j}$ that would connect into the next channel $(2i-2)$, $(j+1)$ (through a barrier overlap) be represented by $t_{i,j} = u_{2i-2,j+1} - u_{i-1,j}$. If the velocity is assumed to not vary along the width of a channel i.e., a flat flow profile, then $\alpha = \frac{t_{i,j}}{w_{i,j}} = \frac{u_{2i-2,j+1} - u_{i-1,j}}{u_{1,j} - u_{i-1,j}}$. Similarly, considering channel $i-1, j$, we can say that $\beta = \frac{u_{i-1,j} - u_{2i-3,j+1}}{u_{i-1,j} - u_{i-2,j}}$.

But the velocity would more accurately represent a parabolic profile inside each channel. Through various revisions, we realised that approximating this as a parabolic flow in a cylindrical pipe gives the least error. Consider the same iteration as above, to calculate the value of α in the case of a parabolic flow profile. We start by considering a cylindrical pipe of radius $w_{i,j}$, and a point T at a distance of $t_{i,j}$ above the centerline. We define α as $\frac{Area\ below\ the\ point\ T}{Total\ area\ under\ the\ curve}$ or $\frac{Area(blue)}{Area(blue) + Area(orange)}$ **(figure S.3A)**. The same calculation holds for β w.r.t channel $i-1, j$. **Figure S.3B** shows the value of n for various exponents, in the case of flat profile and approximated parabolic profile. We can see that the difference in the value of n is significant in the range of [0.33,1] and then decreases as $n > 1$. Further proof of the accuracy of this model can be seen from **figure S4** (discussed in the section 4).

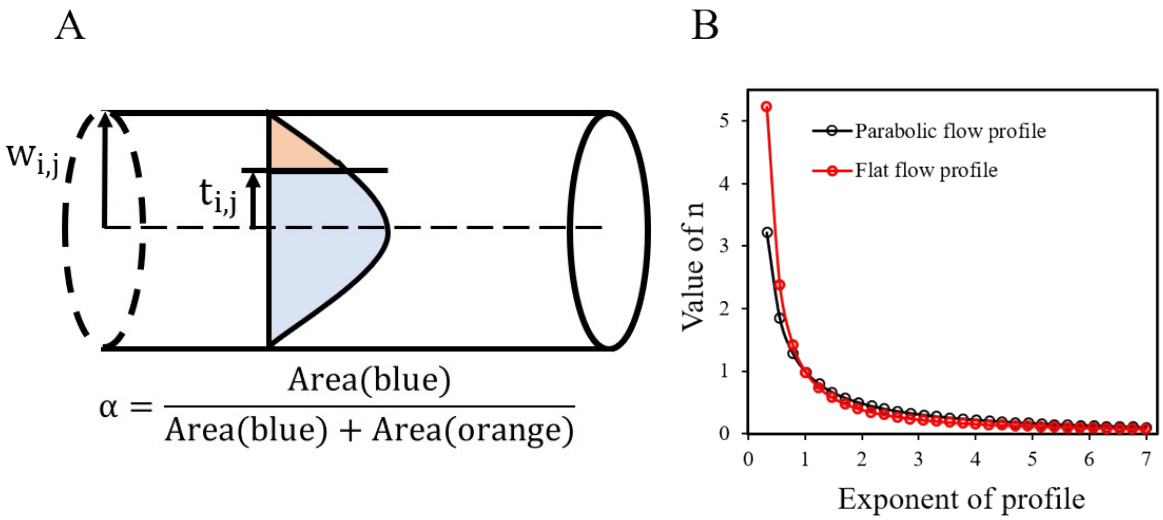

Figure S3: (a) A schematic diagram of the flow through a cylindrical pipe of width $w_{i,j}$. The parabolic variation of velocity inside the pipe is highlighted. The value of α is approximated as $\frac{Area(blue)}{Area(blue) + Area(orange)}$. (b)Variation of value of n with the exponent of the profile for a flat and parabolic flow profile. The flat flow profile approximation shows a significant difference for the range of [0.33,1].

4. Sensitivity of algorithm

To understand the sensitivity of the model, we compare the RMS errors for the extreme cases of $y = x^3$ and $y = x^{0.33}$ as we vary the value of n through $\pm 15\%$ deviation. As seen in **figure S4**, the RMS error minimizes around 0 % deviation, confirming the accuracy of the model. As the value of n changes from the estimated value, corresponding RMS error increases. For both the power functions, the RMS error doesn't go above 0.08 with $\pm 15\%$ deviation. This shows the stability of the model, especially from an experimental stand point.

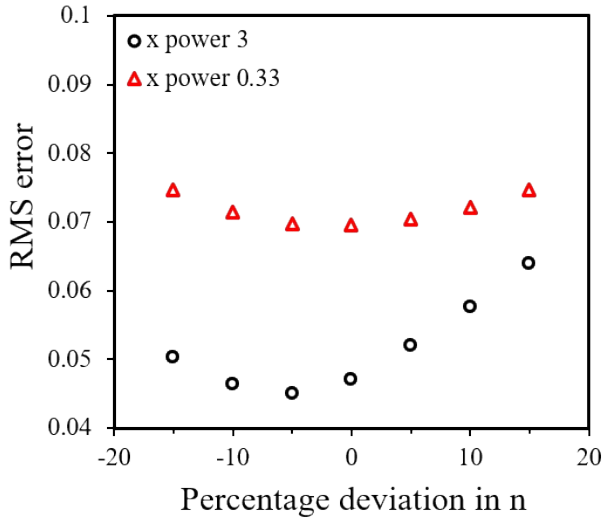

Figure S4: Variation of RMS error with deviation in the value of n in the profiles $y = x^3$ and $y = x^{0.33}$. The RMS error minimizes around 0% deviation from the estimated value of n. The RMS error remains below 0.08 for a deviation of $\pm 15\%$.

Even if the actual flowrate during an experiment varies slightly from the ideal value, the errors don't increase rapidly.

5. Simulation on the experimental device

The device dimensions used for the simulations were different from that used in experiments (as mentioned in the section- *Materials and Methods*). To ensure the flow rates were achievable by the pressure pumps, the experiments were conducted on a device with larger dimensions. Here, we re-evaluated the simulations on the experimental device to ensure that the results achieved translate from simulations to experiments, as intended (**figure S5**).

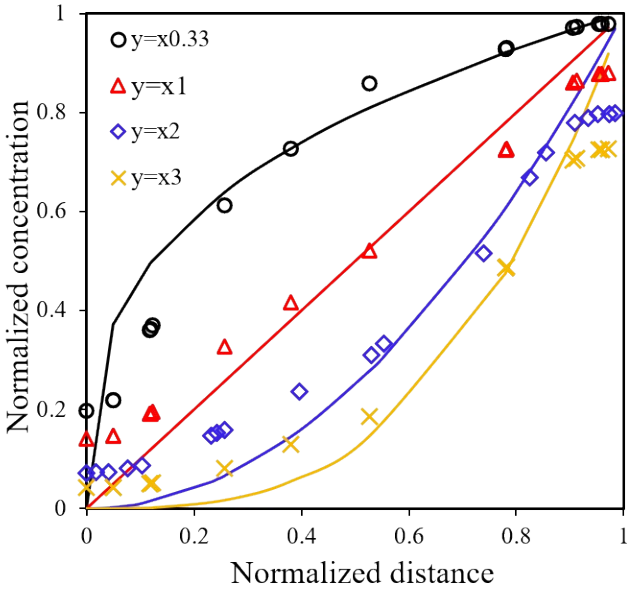

Figure S5: Comparison of simulated gradient profiles ($x^{0.33}$, x^1, x^2 and x^3) with their target functions (solid lines). This simulation was conducted on a device with the exact dimensions of the experimental gradient generator to ensure that the results translate as intended.

6. Supplementary movie

M1. The supplementary movie **M1** compares the pulsating nature of flow between syringe pump and positive displacement pressure pumps. We look at the intersection of level 1 and level 2 for the experimental flow conditions necessary to generate the gradient profile $y = x^2$ (details in the section - *Comparison between the target functions and the experimentally generated gradient profiles*). The video is at speed 1X. The width of the main channel in the video (i.e., channel 2,2) is approx. 400 µm. We note that the flow pulsates highly in the syringe pump experiment in comparison to the pressure pump set up. Thus, we are not able to define a steady state condition to measure the results through syringe pumps.